Astron. Astrophys. 337, 591–602 (1998)

ASTRONOMY AND ASTROPHYSICS

Bolides produced by impacts of large meteoroids into the Earth's atmosphere: comparison of theory with observations

II. Benešov bolide spectra

J. Borovička[1], O.P. Popova[2], A.P. Golub'[2], I.B. Kosarev[2], and I.V. Nemtchinov[2]

[1] Ondřejov Observatory, Astronomical Institute of the Academy of Sciences, CZ-251 65 Ondřejov, Czech Republic
[2] Institute for Dynamics of Geospheres, Russian Academy of Sciences, Leninsky pr. 38, build. 6, 117979 Moscow, Russia

Received 24 February 1998 / Accepted 3 June 1998

Abstract. The unique observational spectrum of the very bright Benešov bolide EN 070591 is compared to theoretical bolide spectra. The -19.5 mag bolide was induced by a meteoroid of an estimated initial mass of 4000 kg, a density of 2 g cm^{-3} and a kinetic energy of 10^{12} J (0.2 kT TNT). The ablating piston model predicts spectra of large bolides by radiative hydrodynamics calculations. We present examples of the calculated H-chondrite vapor spectral opacities and of the resulting spectra for various parameters.

Both theoretical and observed spectra show that bolide radiation is composed of atomic line emissions, molecular bands and continuum radiation. The role of the continuum increases with increasing meteoroid size and with decreasing altitude. The atomic lines are produced under the effective excitation temperature of 4000–6000 K.

The lines of Fe I are too faint and the lines of Ca I are too bright in the model in comparison with the observations. Also the computed continuum level is too high. These differences can be explained by the fact that the vapors occupy a larger volume and have lower density than predicted. This is probably a consequence of a mutual interaction of fragments after the meteoroid fragmentation and of a not well understood ablation process. Other differences between the theory and the observation are described and possible model improvements are discussed.

Key words: meteoroids, meteors

1. Introduction

One of the brightest and well documented bolides detected by the European Network is the Benešov bolide EN070591 (Borovička & Spurný 1996). This bolide proved very useful for the comparison of observational data with the recently created theoretical model of a large meteoroid entry into the atmosphere (Nemtchinov et al. 1994; Golub' et al. 1996a). In Borovička et al. (1998, hereafter Paper I), the bolide dynamics, fragmentation and integral radiation has been analyzed. In this paper we will compare the observed and modeled spectra of bolide radiation. The main goal of the study is the assessment of the Benešov bolide characteristics using the above mentioned theory and checking the validity of the theory.

The main result of Paper I was to conclude that several stage fragmentation of the meteoroid occurred along the bolide trajectory. The bolide had already been significantly decelerated at altitudes between 50–40 km, while enormous luminosity was produced below 40 km. This could be explained by an assumption that the meteoroid was already fragmented into 10–30 pieces each with mass 100–300 kg at altitudes 60–50 km. Some of the primary fragments were fragmented again at altitudes 38–31 km, while more compact fragments were disrupted at 24 km. There are direct observational evidences of the fragmentations below 38 km. The products of the disruption at 24 km were photographed down the altitude of 17 km, where they ceased to be visible. It is probable that several fragments with a mass of the order of few kg reached the ground as meteorites. They were, however, not recovered. The initial mass of the Benešov meteoroid was estimated to 3000–4000 kg and the density to 2 g cm^{-3}. The initial velocity was 21 km s^{-1} (Borovička et al. 1998).

As described in Paper I, two models of meteoroid fragmentation have been proposed. They differ in whether the fragmented body is still taken as a single body with increasing radius after the break-up or the produced fragments are considered as individual bodies. The former model is called a liquid-like or "pancake" model and assumes that all fragments are embedded in a common shock wave with common deceleration and radiation. By fitting the observed deceleration and the light curve of the Benešov bolide it was found that while some fragments undoubtedly escaped from the common motion, large number of pieces formed at 24 km, and also some formed at 38–31 km, justified the liquid-like description.

The study of the bolide spectra can provide further insight into the process of meteoroid ablation, its interaction with the atmosphere and the production of radiation. The theoretical radiative-hydrodynamic model of Golub' et al. (1996a, 1997) is based on the analogy between one-dimensional non-stationary motion of a cylindrical piston in the air and the two-dimensional

Send offprint requests to: J. Borovička (borovic@asu.cas.cz)

quasi-stationary flow around the body. The mass losses are dominated by vaporization due to thermal radiation falling onto the surface of the meteoroid. The model predicts that the spectrum of a large or (and) deeply penetrating body is of a continuum type with superimposed spectral lines.

The observed spectra led Borovička (1993) to propose another model of meteor ablation and radiation. It was assumed that in the relatively dense layers of the atmosphere the surface of a meteoroid is melting, the temperature of the surface being about 2000 K. The liquid, formed by the well melting siderophile elements, is being separated from the body and carries away also small solid particles of the low melting crust formed by the refractory elements. The material is further heated by the surrounding gas of about 4000 K, formed mainly by the hot air and the evaporated material. The atoms of the refractory elements evaporate incompletely or too late, so they are underabundant in the region of the hot gas relatively to the siderophile elements. This may explain the changes in the composition of the emitting region with the altitude. The high temperature (about 10,000 K) component of the spectrum probably originates in the mixing region of the shock heated air and vapor. This region is relatively thin and this may explain its small role in the flux in the observational passband.

Borovička (1993) calculated the spectrum of the emerging radiation under simplified assumptions. His model was based on the observations of not very large meteoroids, e.g. EN 151068 Čechtice with the size of about 10 cm. Air has not been taken into account, only the vapor lines were considered and a uniform temperature distribution in the emitting volume was assumed. Nevertheless, the observed spectrum could be fitted quite well after subtracting the continuous radiation. The size of the volume was found much larger than the meteoroid size, but no theoretical estimates of the volume shape have been done.

The observed spectrum of the Benešov bolide offers a unique opportunity to compare the spectrum of an actual meter sized meteoroid with the theory. The spectrum has already been described and analyzed at selected points by Borovička & Spurný (1996). A multitude of atomic spectral lines dominates the spectrum but a relatively strong continuum is also present at lower altitudes. The absolute majority of atomic lines belongs to the meteoric vapor heated to about 5000 K. The origin of the continuous radiation is less clear. Borovička & Spurný (1996) concluded that the continuum is produced by the same 5000 K vapor. They criticized the air-radiation dominated model of Nemtchinov et al. (1994, 1995), where the shocked air is considered as the primary source of bolide luminosity. However, the addition of the vapor opacity into the model showed that the model predicts the line radiation in qualitative agreement with the observations (Golub' et al. 1996b, 1997). Detailed analysis of the spectra is the goal of this paper.

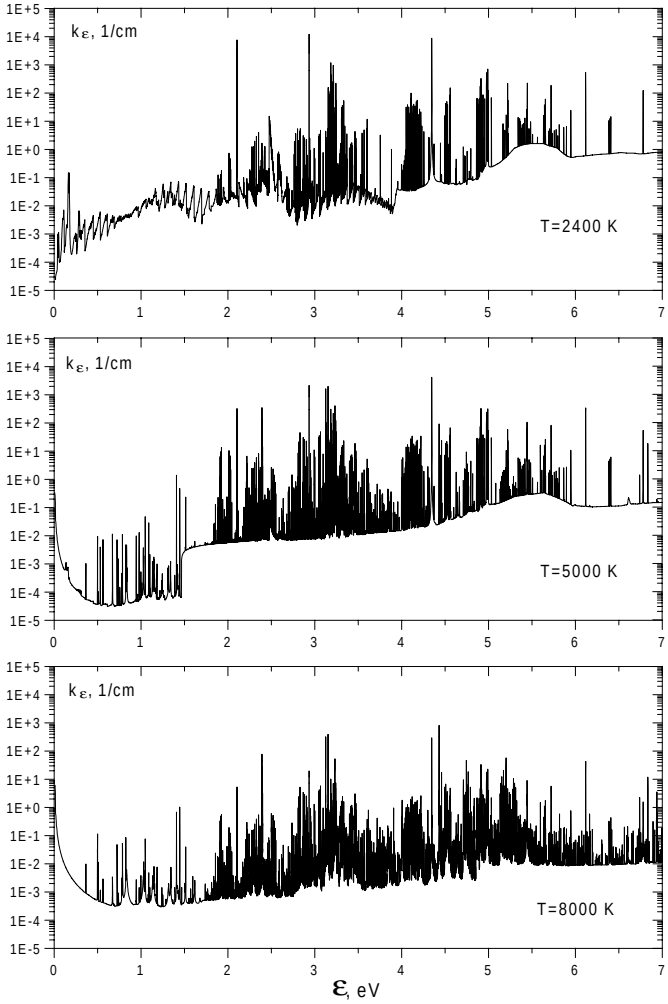

Fig. 1. Spectral opacities for H-chondrite vapor at different temperatures under pressure $P = 10$ bar.

2. The model

In general, the flow pattern around a meteoroid penetrating through the atmosphere or around aerodynamically interacting fragments should be modeled using three-dimensional radiation hydrodynamic codes. However, to obtain the detailed spectral and angular dependencies of the radiation field in the 3D geometry is a formidable task. Moreover, observations do not give us the necessary input data on the sizes of fragments, their relative position, and shape. In case of the Benešov bolide, only a few fragments were resolved spatially (see Paper I). To predict the spectra we will therefore analyze only two limiting cases – individual motion and radiation of one or several fragments and a liquid-like cloud of fragments and vapor with a common shock wave. In both cases we will use the one-dimensional ablating-piston single-body model (Golub' et al. 1996a).

The emerging spectra are determined by conducting radiation-hydrodynamic simulations taking into account ablation and radiation transfer in the air and the meteoric vapor. The local thermodynamic equilibrium is assumed for the gas. In the following we review the spectral opacities used and give examples of the resulting thermodynamic configuration and the emerging spectra. In Paper I, the spectra were integrated over the wavelength providing theoretical luminous efficiencies for meteoroids of various sizes.

2.1. Spectral opacities

The model assumes a strict boundary between the atmosphere and the vapor layer. The opacities of the air and the vapors are therefore taken separately. The air opacities were taken from Avilova et al. (1970) and Romanov et al. (1993). Detailed tables of spectral opacities of chondritic material at different temperatures and densities were computed in Kosarev et al. (1996). The opacity tables were further improved for this work taking into account more chemical elements and increasing the number of wavelength points to describe better the line shapes. The methods of calculation were in general the same as in Kosarev et al. (1996). The main new features are the following:

a) The chemical composition of the chondrite vapor was modeled by 166 chemical compounds arising from a mixture of 10 elements: Fe-O-Mg-Si-C-H-S-Al-Ca-Na. In Kosarev et al. (1996) only the first four elements were taken into consideration. The lines of calcium and sodium proved particularly important in the resulting spectra.

b) Besides O_2, FeO, MgO and SiO the absorption in bands and the continuous spectrum of diatomic molecules CO, CO^+, H_2, MgH, OH, FeH, SiH, SiH^+, CS, SiS, S_2, SO, SH, AlO, AlH, CaO, CaH, NaH, Na_2 was taken into consideration. The data for these molecules have been obtained from different published works, e.g. for the important molecule CaO the work of Hedderich & Blum (1989) was used. Absorption in the infrared bands of MgO was also added (Diffenderfer et al. 1983).

c) The absorption by triatomics H_2O, CO_2, SO_2 was also considered. The cross sections for the water vapor were compiled up to 8000 cm^{-1} from the data found in Young (1977), Soufiani et al. (1985), Hartmann et al. (1984), Phillips (1990). Beyond 8000 cm^{-1} the absorption by the overtone bands was calculated by means of the HITRAN 92 total band intensities (Rothman et al. 1992). The parameters for CO_2 and SO_2 were taken from HITRAN 92 as well.

d) The absorption in the fundamental bands and overtones of the added diatomic molecules was calculated by using the slightly modified just overlapping line approximation (Penner 1959; Sulzmann 1973).

e) The broadening due to the interaction with hydrogen atoms was added in the calculation for the width of the atomic lines (Deridder & Van Rensbergen 1976).

f) The spectroscopic constants for some additional lines of Fe I observed in the Benešov spectra were taken from Nave et al. (1994).

g) The number of points for the photon energy grid was increased up to almost 20,000 (in the "old" tables there were about 10,000 spectral intervals). This allowed us to describe the line emission with better resolution.

The average chemical composition of several types of meteorites was given in Jarosewich (1990). For the modeling of the Benešov radiation we used the H-chondrite composition which is sufficiently close to the composition of other chondrites for our purposes. The H-chondrite abundances (by weight) are: SiO_2 - 36.6%, FeO - 10.3%, MgO - 23.26%, Fe(metallic) - 15.98%, FeS - 5.43%, C - 0.11%, H_2O^+ and H_2O^- - 0.44%, Al_2O_3 - 2.14%, CaO - 1.74%, Na_2O - 0.86%. In addition H-chondrites typically consist of TiO_2 (about 0.12%), CrO_3 (0.5%), MnO (0.3%) and Ni (about 1.6-1.75%). However, Ti, Cr, Mn and Ni have not been included in the calculations of the composition and opacities of the vapor.

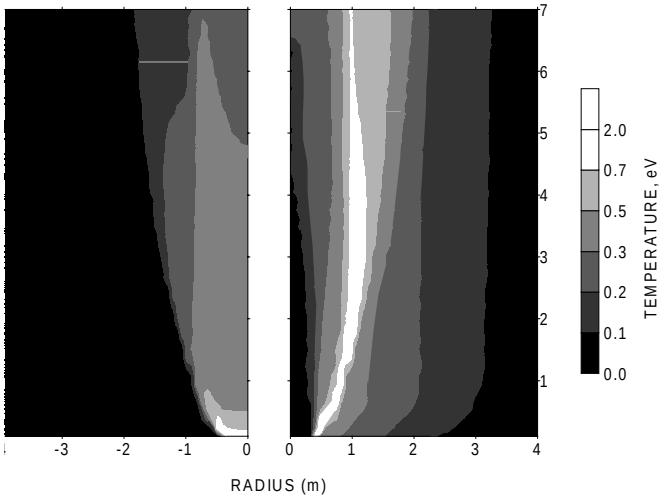

Fig. 2. Distribution of the brightness temperature in the panchromatic passband (left side) and the real temperature distribution (right side) computed in the framework of the ablation model for the body radius 0.42 m, velocity 20 km s^{-1}, and altitude 40 km.

Conserving the proportionality in number of atomic nuclei we obtain the corresponding element fractions in particle number: Fe - 11.484%, O - 51.836%, Mg - 15.428%, Si - 16.287%, S - 1.651%, Al - 0.561%, Ca - 0.830%, Na - 0.371%, C - 0.245%, H - 1.306%. The analysis of the composition of vapor shows that the number fraction of Fe I and Mg I is rather stable at temperatures 4000–6000 K and is close to the above mentioned fractions of these elements. The fraction of Na I, Ca I and Al I substantially decreases at temperatures of about 5000 K due to ionization.

As an example of the dependencies of the absorption coefficients on the photon energy, the results for pressure $P = 10$ bar and several temperatures of the H-chondrite vapor are presented in Fig. 1.

2.2. Thermodynamic configuration

The thermodynamic configuration of the vapor and the atmosphere around the ablating body is a result of the radiation-hydrodynamic simulations. As a typical example we present here the simulations for the H-chondrite body with radius $R = 0.42$ m, velocity $V = 20$ km s^{-1} and altitude of flight $H = 40$ km.

The distribution of the brightness temperature in the panchromatic passband (left side) and the real temperature (right side) versus the radius R and the distance Z from the blunt nose of the meteoroid is given in Fig. 2. In Fig. 3 (upper panel) the maximal temperature of the air ($T_{\rm am}$) and of the vapor ($T_{\rm vm}$) and the maximal brightness temperature ($T_{\rm bm}$) in each cross-section

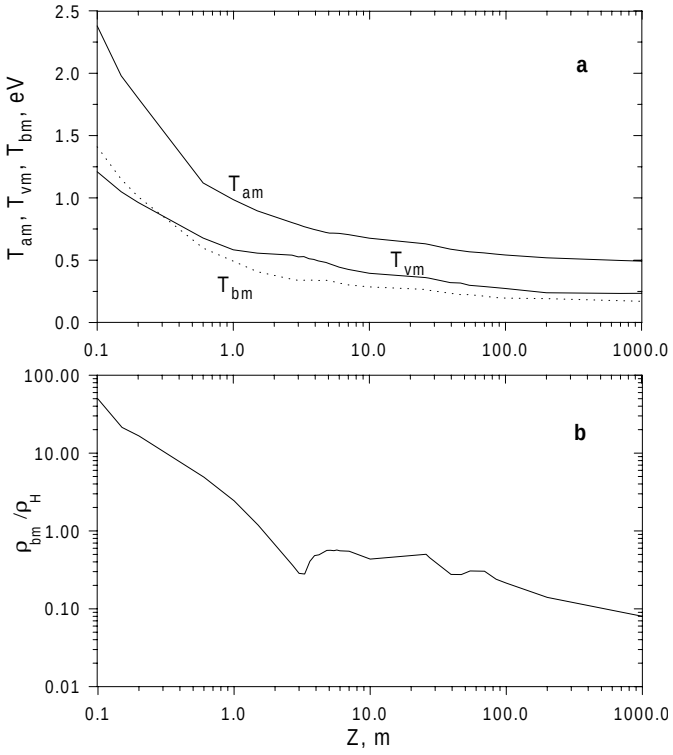

Fig. 3. a Maximal temperature of the air ($T_{\rm am}$), of the vapor ($T_{\rm vm}$) and the brightness temperature in the panchromatic passband ($T_{\rm bm}$) in the cross-section of the bolide versus the distance along the axis Z. **b** The ratio of the density $\rho_{\rm bm}$ at the point of maximum brightness to the undisturbed atmospheric density $\rho_{\rm H} = 4 \times 10^{-6}$ g cm^3.

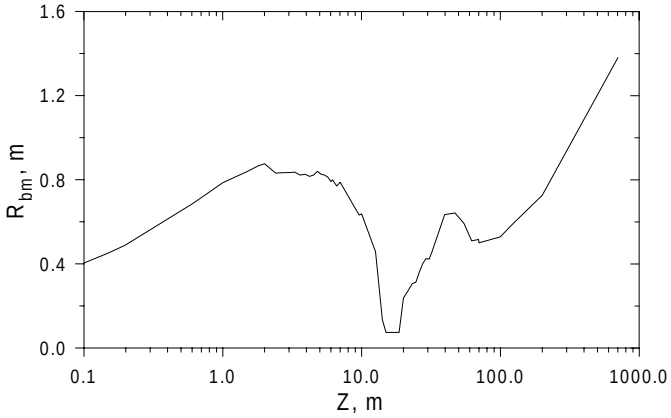

Fig. 4. Radius $R_{\rm bm}$, corresponding to the maximum of brightness temperature in the panchromatic passband in the cross-section of the bolide, versus distance along the axis Z.

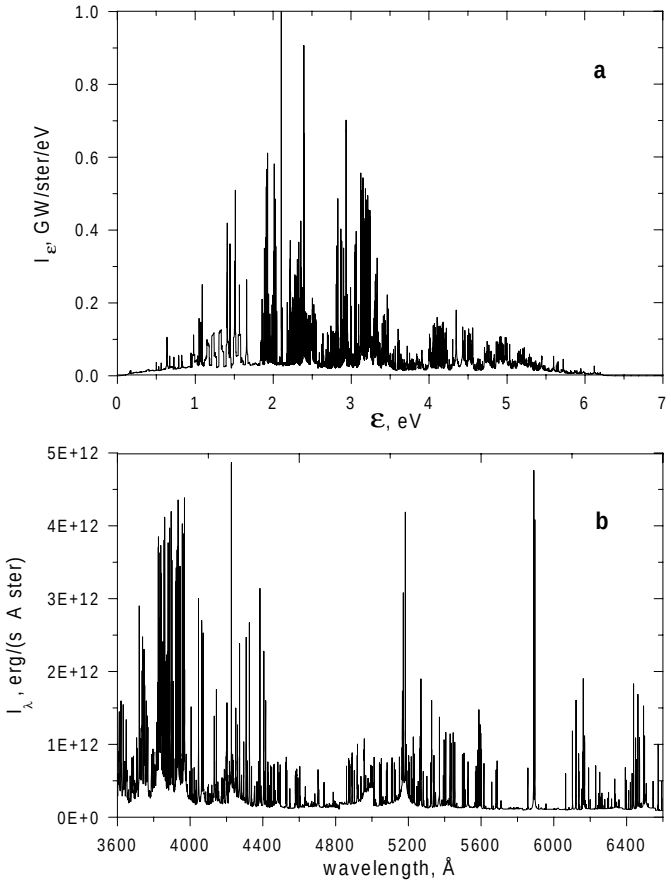

Fig. 5a and b. The theoretical spectrum at altitude 40 km for body radius 0.42 m and velocity 20 km s^{-1}: **a** in whole spectral range, **b** and in the panchromatic passband. The length of the luminous volume was limited by $Z = 200$ m.

are given versus the distance Z. In the lower panel of Fig. 3 the ratio $\rho_{\rm bm}/\rho_{\rm H}$ of the density at the point of maximum brightness to the undisturbed atmospheric density $\rho_{\rm H}$ ($\rho_{\rm H} = 4 \times 10^{-6}$ g cm^{-3} at altitude 40 km) is given. At the distances Z of 2–20 m, where the temperature of the vapor falls down to 0.35–0.55 eV (4000–6000 K) and the radiation is emitted mainly in the visible range, the typical density is about 2×10^{-6} g cm^{-3}. It is interesting to note that the brightness temperature $T_{\rm bm}$ closely follows the vapor temperature $T_{\rm vm}$ and is lower by a factor of two than the air temperature $T_{\rm am}$.

In Fig. 4 the radius $R_{\rm bm}$ corresponding to the maximum brightness temperature $T_{\rm bm}$ in the cross-section is shown. The maximum radius of the volume with the brightness temperature of about 0.4 eV and a density of (1–5)$\times 10^{-6}$ g cm^{-3} is about 0.8 m, i.e. twice the radius of the body. The length of this bright part of the luminous volume is about 2–6 m. The size of the luminous volume in the first approximation is proportional to the size of the body.

2.3. Theoretical spectra of radiation

Theoretical spectra represent the sum of radiation of all regions up to a distance of 200 m behind the body. The radiation is averaged over all directions. The theoretical spectrum for altitude 40 km, meteoroid velocity 20 km s^{-1} and radius 0.42 m is given in Fig. 5a and b. The spectrum in the whole spectral range is shown as a function of photon energy ε (Fig. 5a). It should be noted that large part of the emitted energy is out of the registration passband of photographic networks. The part of the spectrum corresponding to the panchromatic passband is presented in Fig. 5b as a function of wavelength.

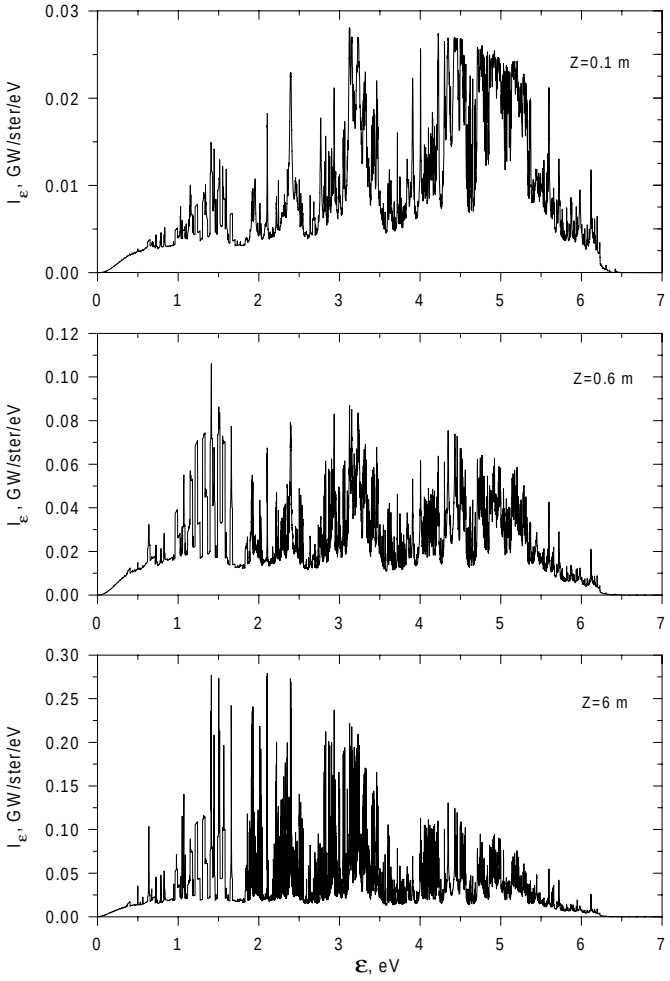

Fig. 6. The theoretical spectra at altitude 40 km for $R = 0.42$ m, $V = 20$ km s^{-1}, and different lengths Z of the luminous volume.

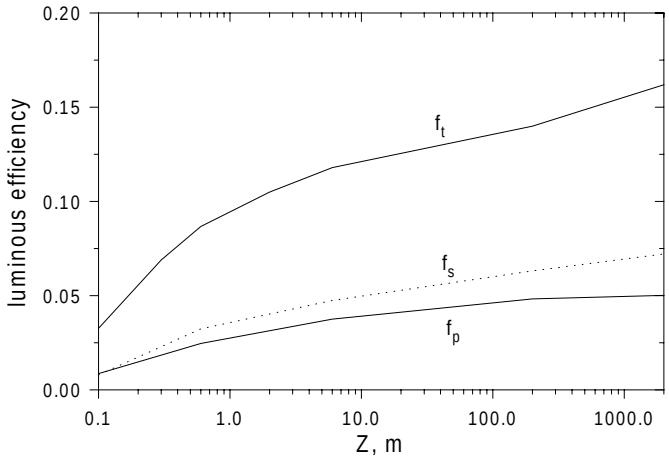

Fig. 7. The fractions of the kinetic energy loss radiated in the whole spectrum (f_t), in the satellite sensor wavelength range (f_s) and in the panchromatic passband (f_p) as functions of the distance Z from the meteoroid nose for $H = 40$ km, $R = 0.42$ m, $V = 20$ km s^{-1}.

The computed spectrum is formed by a superposition of a continuum radiation and emission lines and bands. The maximum of the intensity is reached by several narrow atomic lines in the 1.9–2.6 eV region. However, large amount of energy is emitted by a high continuum level and relatively broad band emissions in the region 0.9–1.7 eV. This region (7000–14,000 Å) is out of the photographic panchromatic passband, but is partly covered by the satellite-based infrared detectors which are sensitive up to 10,500 Å (Tagliaferri et al. 1994). We should underline that the spectrum in the wavelength range of the Satellite Network (SN) sensors, i.e. 1.1–3.1 eV, is substantially different from the spectrum in the panchromatic band and in the visible range. This means that it would be erroneous to use observational data from the ground based photographic systems directly for the calibration of the Satellite Network data and vice versa.

The contribution of different parts of the luminous volume to the total spectrum is demonstrated in Fig. 6. Spectral radiation cut off at some distances Z from the bolide nose is shown. The maximum of the spectra gradually moves from the UV range, i.e. 4.5–5.5 eV at Z = 0.1 m, into the visible and IR range, i.e. 1.5–3.5 eV at Z = 6 m. The role of lines in the spectra increases with the distance Z when new, colder and colder regions are taken into account. The region of the nearby wake at a distance of several diameters of the body, is mainly responsible for the emission in the panchromatic wavelength range, while the bolide's head is mainly responsible for the UV emission, and the far wake for the emission in the IR.

The dependence of the total energy loss radiated in the whole spectrum (f_t), in the wavelength range of the SN sensors (f_s), and in the panchromatic passband (f_p), on the distance Z is given in Fig. 7. The value of f_p shows virtually no change for Z larger than about 20–50 m, while the total losses (f_t) and the output in the SN sensor wavelength range (f_s) continue to grow, since a large amount of energy, mainly in the IR, is emitted by the rather cold part of the bolide. The total energy losses exceed the output in the panchromatic wavelength range by a factor of three.

The dependence of the theoretical spectra on altitude and meteoroid size will be discussed in Sect. 4.2 in connection with a comparison to the observed spectrum.

3. The observed spectrum

The observed spectrum of the Benešov bolide was described by Borovička & Spurný (1996). Here we repeat the basic facts with the emphasis on the instrumental effects which are important for a comparison with the theoretical spectra.

The spectrum was photographed on two plates and covers the trajectory of the bolide from an altitude of 90 km to 19 km. The wavelength range is given by the sensitivity of panchromatic material, i.e. 3600–6750 Å. The dispersion is 50–70 Å mm^{-1} in the first order spectra. Unfortunately, the blue part of the spectrum was not well focused. At some altitudes the blurred section extends up to 4500 Å. The use of the second order spectra can sometimes make the situation better.

Even in the well focused parts, the spectral resolution is limited. Individual emission lines exhibit an instrumental pro-

file with the width much larger than the natural width of the lines. Apart from the limited resolution of the spectrograph, the reason may be the detection of the true geometrical extent of the radiating volume. The instrumental profiles were well described by a Gaussian function with a width of 3–5 Å.

The measured spectra were corrected to the spectral sensitivity of the spectrograph. However, absolute calibration was not possible from the spectral records alone. We used a direct image of the bolide taken at another station to determine the bolide absolute magnitude as a function of altitude. The spectrum was then scaled to obtain the luminosity in ergs s^{-1} $ster^{-1}$ $Å^{-1}$ consistent with the derived magnitude.

The spectrum consists of atomic emission lines, molecular bands and continuum radiation. The following species have been identified: Fe I, Na I, Mg I, Al I, Ca I, Ca II, Ti I, Cr I, Mn I, Ni I, Li I, N II, Si I, Si II, Co I, MgO, AlO, CaO, and FeO. The line spectrum was analyzed at selected altitudes in Borovička & Spurný (1996) by the method of Borovička (1993). It was concluded that the majority of the lines and the continuum can be fitted by a model containing the radiation of meteoritic vapors heated to 4000–5000 K. Some additional effects were also found. They are briefly listed here:

- The abundance of calcium was found to be very low in the upper part of the trajectory. This was ascribed to the effect of incomplete evaporation.
- Very strong radiation from the bolide wake is present at altitudes of 70–55 km. The wake spectrum cannot be described in terms of thermal equilibrium. Low excitation intercombination lines are very strong.
- Relatively weak lines of ionized silicon are present at altitudes of 75–40 km. These lines exhibit short flares and can be ascribed to the high temperature (10,000 K) spectral component. Surprisingly, at altitudes of 65–57 km, the Si II flares are accompanied by flares of ionized nitrogen lines which cannot be explained even by the high temperature component.
- A persistent radiating cloud was detected near the position of the bolide brightest flare at 24 km. The spectrum of the cloud consists almost exclusively of a continuum and molecular bands.
- Thermal continuum from the meteoroid surface was registered at the beginning of the event.

In the next section we will compare the observed spectra at altitudes 63.5 km, 40 km and 24.5 km with the theoretical spectra.

4. Comparison of the theoretical and observed spectra

Before making the comparison we must set the theoretical spectra to the same resolution as the observed spectra. This was done by the convolution of the theoretical spectra with the Gaussian profile:

$$I(\lambda) = (\sqrt{\pi}\Delta)^{-1} \int_{\lambda-3\Delta}^{\lambda+3\Delta} J(\lambda') \exp\left\{[(\lambda-\lambda')/\Delta]^2\right\} \mathrm{d}\lambda', \quad (1)$$

where $J(\lambda)$ is the theoretical spectrum, $I(\lambda)$ is the convoluted spectrum and Δ is the width of the Gaussian profile.

The spectra were computed for altitudes of 60 km, 40 km and 25 km. They are compared with the observed spectra in Figs. 8–10. The instrumental width Δ was 3 Å at 60 and 40 km and 5 Å at 25 km. Since the velocity of the bolide at all altitudes is well known (approximately 20 km s^{-1} at 60 and 40 km and 15 km s^{-1} at 25 km) and the meteoroid composition was very probably not far from that of an H-chondrite, the only free parameter of the model is the meteoroid radius. We computed the spectra for fixed radii of 1.4 m, 0.42 m, and, at 25 km, also 0.14 m. The observed luminosity can be attained either by one large body or by a number of smaller bodies. We first evaluate the possible meteoroid radii from the total radiated intensity and then we will discuss the details of the spectra.

4.1. Total intensities, scaling laws

The assessment of the meteoroid radius from the bolide luminosity is a process analogous to the radiative radius approach used in Paper I. However, here we compare calibrated spectra in a well defined wavelength range and no doubts therefore arise because of the transformations of different magnitude systems.

In Table 1, the integral intensity (erg s^{-1} $ster^{-1}$) in the wavelength range 4500–6600 Å, where the observed spectra were in good focus, and in a wider passband are given for three altitudes. The theoretical integral intensity increases between the altitude of 60 and 40 km by a factor of about 15, while the air density increases by a factor of 13.4. With the increase in the radius of the body from 0.42 to 1.4 m (R^2 changes by a factor of 11.1) the intensity of the emitted radiation increases by a factor of about 12. Similar relations exist at altitudes 40 and 25 km. We will assume in the next simple estimates that the radiation intensity is proportional to the air density and to the square of the radius.

When comparing the observed intensity at 63.5 km with the theoretical data for 60 km (a factor of 1.5 in the air density), we see that the observed intensity corresponds to the body radius of about 0.7 m. For a density of 2 g cm^{-3} this gives a mass of 3000 kg, which is at the lower limit of our estimate of the initial mass from the progressive fragmentation model (see Paper I).

At altitude 40 km, the radius needed to explain the luminosity is 1.2 m (15,000 kg of mass). However, the meteoroid was already fragmented at this altitude. The luminosity can alternatively be explained by 8–10 individual fragments with a radius of 0.42 m (see Table 1), giving a total mass of 5000–6200 kg. The dynamic mass of the leading fragment at this altitude (Paper I) is, however, only 300 kg (radius of 0.33 m), so a larger number of smaller fragments probably existed.

The situation is even more complicated at 24.5 km. This is just before the main flare at 24.3 km and the bolide is very bright here. The luminosity could be formally explained by a single body of 1.3 m radius, 13 fragments of 0.42 m radius or about 180 fragments of 0.14 m radius (23 kg). In all cases, however, the total mass is too large, ranging from 18,000 kg to 4000 kg. The mass participating in the main flare was estimated to be no more than 1500 kg in Paper I. The explanation may be

Table 1. Direct comparison of the modeled and observed intensities in a given passband at various altitudes and for different meteoroid sizes.

λ_1–λ_2	$I_{\rm mod}$, erg/s/sr	$I_{\rm obs}$, erg/s/sr	$I_{\rm obs}/I_{\rm mod}$
$H = 60$ km, $V = 20$ km s^{-1}, $R = 0.42$ m			
3700–6600 Å	$0.546\times10^{+14}$	$0.995\times10^{+14}$	1.8
4500–6600 Å	$0.261\times10^{+14}$	$0.500\times10^{+14}$	1.9
$H = 60$ km, $V = 20$ km s^{-1}, $R = 1.4$ m			
3700–6600 Å	$0.657\times10^{+15}$	$0.995\times10^{+14}$	0.15
4500–6600 Å	$0.292\times10^{+15}$	$0.500\times10^{+14}$	0.17
$H = 40$ km, $V = 20$ km s^{-1}, $R = 0.42$ m			
3900–6600 Å	$0.579\times10^{+15}$	$0.465\times10^{+16}$	8.0
4500–6600 Å	$0.369\times10^{+15}$	$0.378\times10^{+16}$	10.2
$H = 40$ km, $V = 20$ km s^{-1}, $R = 1.4$ m			
3900–6600 Å	$0.798\times10^{+16}$	$0.465\times10^{+16}$	0.58
4500–6600 Å	$0.517\times10^{+16}$	$0.378\times10^{+16}$	0.73
$H = 25$ km, $V = 15$ km s^{-1}, $R = 0.42$ m			
4200–6500 Å	$0.151\times10^{+16}$	$0.192\times10^{+17}$	12.7
4500–6500 Å	$0.121\times10^{+16}$	$0.169\times10^{+17}$	13.9
$H = 25$ km, $V = 15$ km s^{-1}, $R = 1.4$ m			
4200–6500Å	$0.219\times10^{+17}$	$0.192\times10^{+17}$	0.88
4500–6500Å	$0.175\times10^{+17}$	$0.169\times10^{+17}$	0.97
$H = 25$ km, $V = 15$ km s^{-1}, $R = 0.14$ m			
4200–6500Å	$0.111\times10^{+15}$	$0.192\times10^{+17}$	173
4500–6500Å	$0.906\times10^{+14}$	$0.169\times10^{+17}$	187

that catastrophic fragmentation had already begun at 24.5 km and so we are dealing with one or more clouds of fragments with an average density much lower than the bulk density of the meteoroid.

Therefore, by comparing the radiated energy in wide passbands, we conclude that meteoroid fragmentation severely affected the Benešov bolide radiation at an altitude of 25 km and also at 40 km. This is in accordance with our progressive fragmentation modeling performed in Paper I. Next we compare the shape of the spectra.

4.2. The shape of the spectra

In Figs. 8, 9, and 10, the theoretical and observed spectra at the altitudes of 60 km, 40 km, and 25 km, respectively, are given. Only the wavelength range where the observed first order spectrum is in sufficiently good focus is shown. Two computed spectra are given for each altitude, one for a single body with a radius of 1.4 m and one for a number of smaller bodies.

Both theoretical and observed spectra consist of a superposition of continuum radiation and atomic line radiation with an additional component from molecular bands. There are, however, differences in the number of lines and their strength relative to the continuum level. When comparing the computed spectra for the 1.4 m body we see a clear tendency for the decreasing of the role of lines and an increasing role for the continuum with decreasing altitude. The same tendency is present in the observed spectra where the continuum level is much higher at 24.5 km than at larger altitudes. However, the role of the lines is significantly higher at all altitudes in the observed spectra than in the 1.4 m spectra.

Decreasing the size of the body leads to an increase of the line radiation in the computed spectra, especially at lower altitudes. In this sense, the computed spectra of a large number of independent small bodies are closer to the observations at 40 km and 25 km than the spectrum of a single large body. This is in agreement with our conclusions from the total radiated intensity. However, significant differences in the theoretical and observed line radiation still remain. They are discussed in detail in the next section.

The shape of the continuum is similar in the observed and computed spectra. The observations show a very flat continuum at all altitudes in the given wavelength range. The theoretical spectrum for a 1.4 m body at 25 km shows a blue continuum but a 0.14 m body at the same altitude has flat continuum. At higher altitudes all computed spectra exhibit flat continua.

The continuum bears little information regarding its origin and it is difficult to say whether it is produced mostly by the vapor or by the air. In this respect the line radiation offers more possibilities for an analysis.

4.3. The line and band radiation

The number of lines included in the theoretical computations is large. For Fe I as many as 1717 lines were taken into account, even though some of them have rather low oscillator strength. On the other hand, such elements as Mn, Ti, Cr and Ni and molecular bands of oxides such as MnO and TiO_2 have not been taken into account as yet.

If we ignore the above elements Mn–Ni, the comparison of the atomic lines in the observed and computed spectra shows that, despite of different intensities, the same lines are generally present in both spectra. All predicted atomic lines are present in the observed spectrum. Some of them are identified in Figs. 8–10.

Of the lines present in the observed spectrum but not in the theoretical spectrum, the most important are the Si II lines (6347 and 6371 Å). They belong to the second, high temperature spectral component and are visible at 63.5 km and weakly at 40 km. The theoretical spectra do not contain this line though temperatures of about 10,000 K are predicted to be present in the model (Fig. 3). Also, no atmospheric lines (i.e. lines of nitrogen or oxygen) are present in the computed spectra. In particular, the

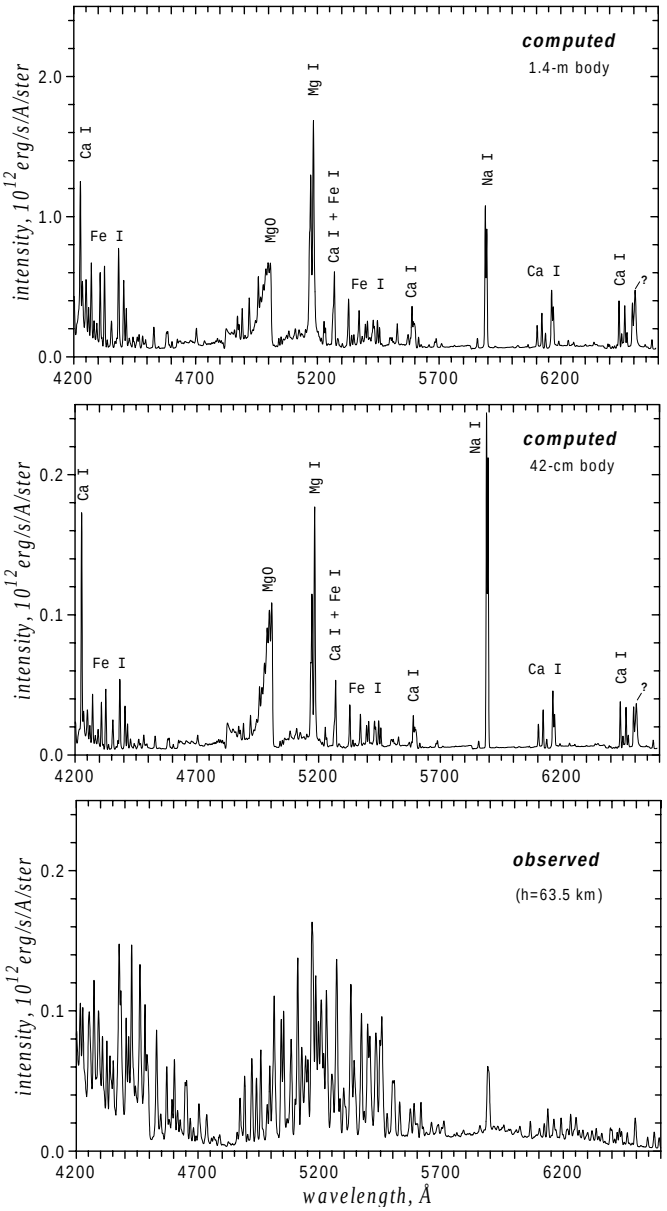

Fig. 8. Comparison of the observed spectrum at altitude 63.5 km and the modeled spectra for meteoroid radii 0.42 m and 1.4 m at altitude 60 km and velocity 20 km s^{-1}. Note the different scale for 1.4 m.

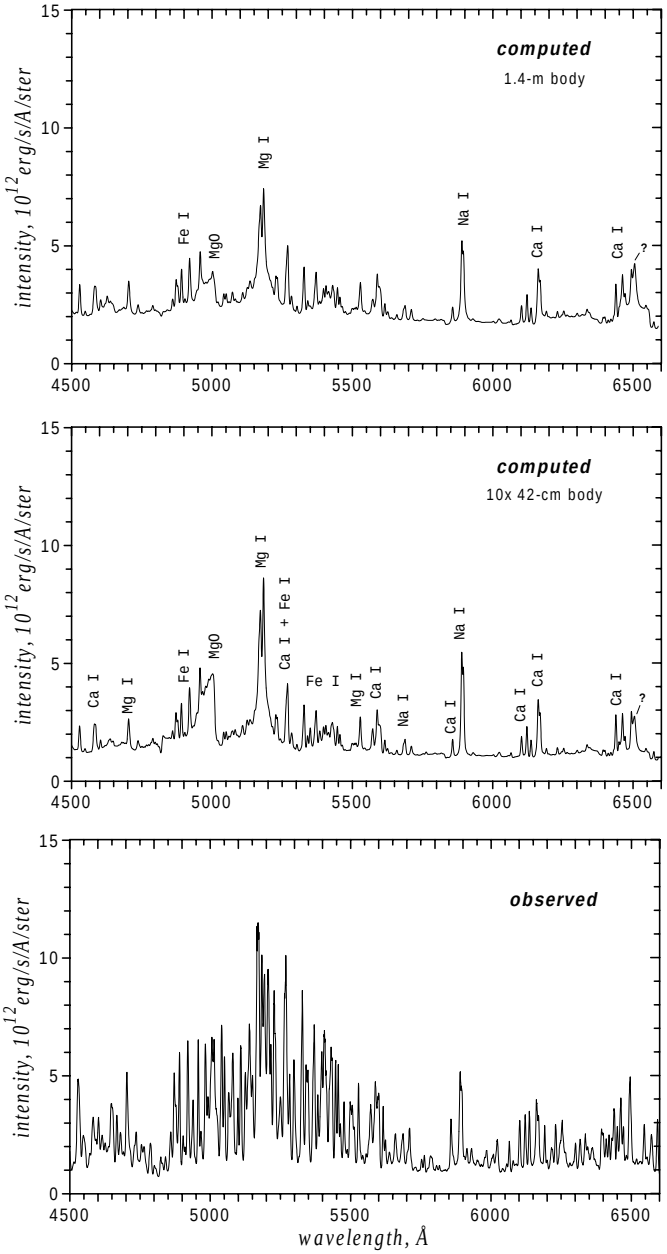

Fig. 9. Comparison of the observed spectrum at altitude 40 km and the modeled spectra for 10 independent fragments with radii 0.42 m and one single body with radius 1.4 m at the same altitude. The velocity is 20 km s^{-1}.

oxygen triplet at 6156–6158 Å, which is observed in fast meteors, is not present. This is in accordance with the observations (except of the peculiar N II lines) but somewhat surprising owing to the importance of the shocked air radiation in the model. The absence of Si II and of the air lines in the theoretical spectrum is explained by the presence of a dense vapor layer in the model. The cooler vapors are supposed to absorb the hot radiation originating from the vicinity of the bolide nose.

The intensities of the lines which are both observed and predicted are often different. The theoretical spectra are dominated by the lines of Mg I, Ca I and Na I, while the lines of Fe I are much fainter than in the observed spectra. Since the Fe I lines are very numerous this causes the different appearance of the line spectra.

To go deeper into the problem, both the observed and the theoretical spectra at 40 km have been analyzed (after subtracting the continuum and the band emissions) by the method of Borovička (1993). The method computes the effective excitation temperature and the column densities of individual atomic species from the line intensities. Of course, neither the theoretical nor the real spectrum are produced at a single temperature. But Borovička (1993) has shown that the single-temperature

Table 2. The analysis of the theoretical and observed spectra of the Benešov bolide at altitude 40 km. The precision of the effective temperature is about ± 300 K, other parameters have been determined within a factor of 2–3.

	1.4 m body	10× 42 cm body	observed
effective excitation temperature (K)	6100	6100	5100
column density of Fe I atoms (cm^{-2})	$4\times10^{+15}$	$4\times10^{+15}$	$7\times10^{+16}$
effective emitting area (m^2)	1400	10×170	12000
Ca I/Fe I	10^{-2}	10^{-2}	10^{-3}
Na I/Fe I	10^{-2}	10^{-2}	10^{-3}
Mg I/Fe I	0.6	0.7	1.1

assumption can describe a meteor spectrum relatively well for not very fast bolides.

The results for the Benešov bolide at 40 km are given in Table 2. The effective excitation temperature of 5100 K was obtained for the observed spectrum. The theoretical spectra gave a temperature 1000 K higher but we do not consider this as a significant difference. More important is the difference in the column density of Fe I atoms. The observed spectrum yields more Fe I atoms along the line of sight by an order of magnitude. The presence of a large number of Fe I lines in the observed spectrum is a demonstration of this fact. On the other hand, the theoretical spectra give larger ratios of Ca I and Na I to Fe I by an order of magnitude. This is the reason why the lines of Ca I and Na I are so conspicuous in the theoretical spectra, although the intensity of Na I lines is in fact not significantly larger than their observed intensity.

The situation at other altitudes is similar but there are also some differences. At 63.5 km, the wake was very strong and many of the bright lines in the observed spectrum originate in the non-equilibrium wake. The theoretical model, however, assumes local thermal equilibrium and cannot reproduce the wake spectrum. At 25 km, on the other hand, the agreement between the observation and the theoretical model is the best, though the Fe I lines are still underestimated. We included the computed spectrum for a 0.14 m body in Fig. 10. The 0.42 m spectrum is something between the 0.14 and 1.4 m spectra and is comparably good in comparison with the observations as the 0.14 m spectrum.

There are also molecular bands in the spectra. The MgO band near 5000 Å is one of the brightest features in the theoretical spectra. In the observed spectra, though present, it is much fainter. The MgO radiation is predicted to originate in the wake. Other molecules identified in the observed spectrum, FeO, CaO, and AlO, have extended band systems and do not form bright features neither in the observed nor in the computed spectra.

The theoretical spectra exhibit an apparent band radiation near 6504 Å which is not observed. It seems that the feature is produced by an interpolation error in the opacity tables but we were unable to identify the source of the error.

5. Discussion

We will now summarize the agreements and disagreements between the predicted and the observed spectra. There is agreement that the spectrum of a large and deeply penetrating bolide is generated by a superposition of thermal continuum, molecular emission bands and atomic emission lines. The general shape of the continuum in the panchromatic region, i.e. nearly no dependence on wavelength, is also confirmed. All predicted atomic lines are present. Finally, the effective excitation temperature as determined from the atomic lines is about 5000–6000 K in both predicted and observed spectra (the main component).

The major difference is the lower column density of the Fe I atoms and the high ratios of Ca I/Fe I and Na I/Fe I in the theoretical spectra. The ratios can be explained by a different degree of ionization. Both calcium and sodium have low ionization potentials and their low abundance in the observed spectrum is explained by their high ionization. The effect of incomplete evaporation of calcium is of minor importance here. A higher ionization for the same temperature means a lower density. The column density of Fe I is, however, higher. It seems that there is more vapor in the radiating region but with lower density, so the radiating region must be much larger than modeled.

The lower density can also explain the lower continuum level because a large part of the continuum is produced by free-free emission and this grows with the square of density. A lower optical thickness of the continuum could also allow the radiation produced by the Si II lines in the vicinity of the shock wave not to be absorbed and to be present in the spectrum.

It seems that a substantially larger volume occupied by the radiating vapor would explain most of the differences between the theoretical and the observed spectra. Indeed Borovička & Spurný (1996) interpreted the Benešov spectrum as being produced in a cylinder of a diameter about 20 meters, i.e. at least 10 times the diameter of the body. We therefore computed the spectrum of a 10 m wide layer of vapors with a temperature of 5000 K and a density of 10^{-7}–10^{-6} g cm^{-3}. The same spectral opacities as for the modeled spectra were used. The shape of the resulting spectrum proved to be closer to the observation.

However, the gas dynamical modeling shows that all vapor in the vicinity of the body must be confined by the shock wave and the diameter of the allowed region is no more than twice the diameter of the body (see Fig. 2). From the gas dynamics point of view, it is impossible to produce a 20 meter diameter vapor region in the vicinity of a 2 meter diameter single body. The sum of a number of individual smaller bodies produces spectra closer to the observation than a single body but still worse than an extended cloud of vapors.

Again, meteoroid fragmentation seems to be the most plausible explanation of this discrepancy. If the bolide is formed not

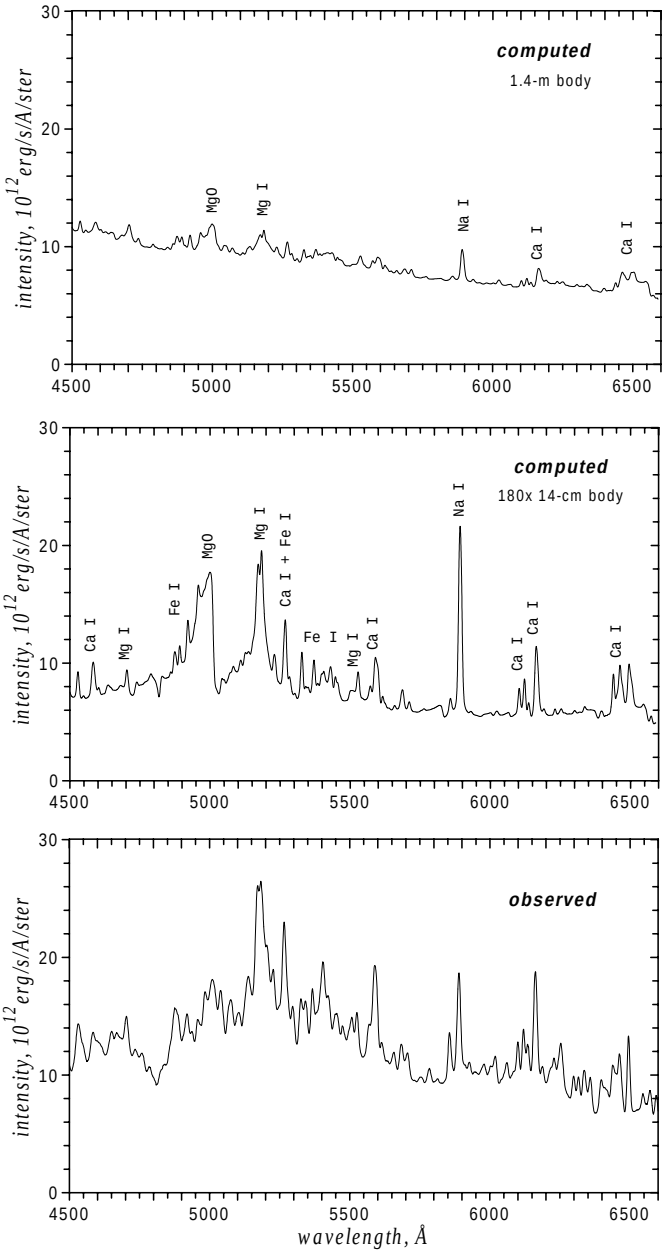

Fig. 10. Comparison of the observed spectrum at altitude 24.5 km and the modeled spectra for 180 independent fragments with radii 0.14 m and one single body with radius 1.4 m at altitude 25 km. The velocity is 15 km s^{-1}.

by a single big body but by a swarm of bodies separated by several meters, the interaction between the shock waves and the vapor may lead to the formation of a common radiating volume at some distance from the head of the bolide. The interaction process has been investigated by Artem'eva & Shuvalov (1996) for 17–27 fragments. The shape of the luminous volume becomes more like a cylinder with the ratio of the radius to the length larger than for a single body with the summary mass. Of course, the radius depends on the distance between the fragments. However, we cannot use the results of these simulations for a more detailed analysis of the spectra as the radiation has not been included into the model yet.

Although the fragmentation is certainly important, the problem with the size of the luminous volume is also present at altitudes around 60 km, where the meteoroid was probably not fragmented. We have to consider the possibility that the main radiating region does not surround the body but is located behind the body. This might occur, if the material is ablated from the body in the form of tiny solid fragments or liquid drops and evaporated later. The vapor then tends to fill the cavern formed by the rarefied wake of the main body and the vapor volume increases and the density decreases. This has been confirmed by a 2D purely hydrodynamic simulation (V.V. Shuvalov, personal communication). More detailed 2D radiation hydrodynamic simulations of such a scenario should be conducted and the resulting spectrum should be compared with observations.

There also remains the question of the primary mechanism which drives the ablation and excitation of radiating atoms. Whether it is the radiation of the shock wave as supposed in many theoretical papers, e.g. Nemtchinov et al. (1994), or the thermal collisions in the hot gas as supposed by Borovička (1993), or both. In the theoretical model under consideration (Golub' et al. 1996a) both mechanisms are actually acting. The first one (radiation) dominates for large bodies or (and) at low altitudes, the second (collisions, or molecular and electronic thermal transfer) dominates at high altitudes and for small bodies. The observed spectrum does not resolve the question of which mechanism dominated in the Benešov case because the 5000 K vapors can be formed both ways and the exact origin of the continuum is not clear. Moreover, there is another mechanism, a turbulent heat transfer, which should additionally be taken into account in the future.

Some observed features are beyond the scope of the present model. The wake radiation at high altitudes needs non-equilibrium modeling. For the description of the persistent radiating cloud at the position of the bright flare at 24 km the quasi-stationary ablating piston model should be replaced by a non-stationary model of an expanding cloud. The recombination of "reexisting" molecules of oxides and an additional oxidation of metals by the air due to turbulent diffusion should be taken into account.

The spectral analysis of the Benešov bolide confirmed the important role of meteoroid fragmentation revealed already from the analysis of the dynamics and light curve in Paper I. Moreover, it was shown that the radiation is not produced by individual independent fragments but by a more complicated configuration. The details of the ablation mechanisms both before and after the fragmentation and the mutual interaction of the fragments are essential for the description of the radiation. This is important not only for the understanding of the meteoroid-atmosphere interaction but also for the derivation of the mass, density, structure and composition of meteoroids from the observation of bolides. The Benešov-like meteoroids are intermediate in size between smaller meteoroids where the conventional analysis gives reliable results (e.g. Ceplecha 1996, Ceplecha et

al. 1996) and very large meteoroids where the simple pancake model may probably be a usable approximation.

Our physical model requires further improvement. First, the model probably underestimates the ablation rate from the rough surface of real meteoroids with non-uniform structure (Popova & Nemtchinov 1996). Second, the model underestimates the role of the kinetic energy of small fragments and liquid droplets thrown away from the rough surface of the meteoroid. Third, turbulent diffusion of the vapor in the air increases the size of the volume occupied by the vapor and decreases vapor density. All these factors should be more correctly incorporated into future theoretical models and codes. We do not anticipate that all these factors may qualitatively change our general description of the Benešov meteor phenomenon and our estimates of the meteoroid mass.

6. Conclusions

Theoretical spectra of radiation from a $\sim$1 meter size H-chondrite meteoroid penetrating the atmosphere at the altitudes of 60–25 km were presented. The spectra are based on the ablating piston model by Golub' et al. (1996a) with improved spectral opacities. The spectra in the wavelength range 4500–6600 Å were compared with the observed spectra of the very bright Benešov bolide EN 070591.

Both the theoretical spectra and the observed spectra have shown that the bolide radiation is composed of atomic line emissions, molecular bands and a continuous radiation. The role of the continuum relative to the lines increases with increasing meteoroid size and decreasing altitude. This is the reason why the continuum is negligible in fainter meteors.

The total radiated intensity in the given passband as well as the shape of the spectrum confirm that the Benešov meteoroid was already fragmented at an altitude of 40 km. This is in agreement with the conclusion of Paper I, where the bolide dynamics and light curve were analyzed.

The atomic lines are produced under an effective excitation temperature of 4000–6000 K in both theoretical and observed spectra. The observed spectrum also contains lines of Si II and N II which must be produced under substantially higher temperatures. These lines are not present in the theoretical spectra although a high temperature region is present in the model. This is due to the fact that the radiation from the hot region is absorbed by the cooler vapors in the model.

The intensities of the lines forming the $\approx$ 5000 K radiation are different in the theoretical model and in the observation. The lines of Fe I are too faint and the lines of Ca I are too bright in the model. Also the continuum level is larger in the model. These differences can be explained by the fact that the vapors are confined in too small volume and under too large density in the model in contrast to the reality. The larger expansion of vapors than predicted is probably a consequence of mutual interaction of fragments and a more complicated ablation process of individual fragments. These effects are to be considered in future modeling.

The theoretical spectra predict that a large part of energy is radiated in the infrared part of the spectrum, especially by the bands of hot air. This could not be confirmed because infrared spectra of Benešov are not available. In the visible region atmospheric emissions are neither predicted nor observed (except for the peculiar N II lines). Similarly, it could not be definitely resolved whether the observed continuum is produced by the vapors or the air.

In summary, we presented the first detailed comparison of a purely theoretical radiative-hydrodynamic spectral model and the observed spectrum of a bolide. The spectra generally agree in respect to the presence of continuous radiation and atomic and molecular emissions. The effective temperature of the atomic emissions and the shape of the continuum are nearly the same. Details of the spectra differ and this is a consequence of poorly known details on the energy transport, ablation, and fragment interaction. Nevertheless, together with the modeling in Paper I, we obtained a consistent picture of the Benešov bolide, including its mass, dynamics, fragmentation and radiation.

Acknowledgements. This work is supported by the Grant agency of the Czech Republic (project no. 205-97-0700) and by Sandia National Laboratories.

References

Avilova I.V., Biberman L.M., Vorob'ev V.S. et al., 1970, In: Biberman L.M. (ed.), Opticheskie svoistva goryachego vozducha (Optical Properties of Hot Air), Nauka, Moscow
Artem'eva N.A., Shuvalov V.V., 1996, Shock Waves 5, 359
Borovička J., 1993, A&A 279, 627
Borovička J., Spurný P., 1996, Icarus 121, 484
Borovička J., Popova O.P., Nemtchinov I.V., Spurný P., Ceplecha Z., 1998, A&A 334, 713 (Paper I)
Ceplecha Z., 1996, A&A 311, 329
Ceplecha Z., Spalding R.E, Jacobs C., Tagliaferri E., 1996, Luminous efficiencies of bolides. In: Maclay T.D., Allahdadi F.A. (eds.) Characteristics and Consequences of Orbital and Natural Space Impactors, Proceedings of SPIE Vol. 2813, p. 46
Deridder G., Van Rensbergen W., 1976, A&AS 23, 147
Diffenderfer R.N., Yarkony D.R., Dagdigian P.J., 1983, J. Quant. Spec. Rad. Transf. 29, 329
Golub' A.P., Kosarev I.B., Nemtchinov I.V., Shuvalov V.V., 1996a, Solar System Res. 30, 183
Golub' A.P., Kosarev I.B., Nemtchinov I.V., Popova O.P., 1996b, Meteoritics 31, A52 (Supplement)
Golub' A.P., Kosarev I.B., Nemtchinov I.V., Popova O.P., 1997, Solar System Res. 31, 85
Hartmann J.M., Di Leon R. Levi, Taine J., 1984, J. Quant. Spec. Rad. Transf. 32, 119
Hedderich H.G., Blum C.E., 1989, J. Chem. Phys. 90, 4660
Jarosewich E., 1990, Meteoritics 25, 323
Kosarev I.B., Loseva T.V., Nemtchinov I.V., 1996, Solar System Res. 30, 265
Nave G., Johansson S., Learner R.C.M., Thorne A.P., Brault J.W., 1994, ApJS 94, 221
Nemtchinov I.V., Popova O.P., Shuvalov V.V., Svetsov V.V., 1994, Planet. Space Sci. 42, 491
Nemtchinov I.V., Popova O.P., Shuvalov V.V., Svetsov V.V., 1995, Solar System Res. 29, 133

Penner S.S., 1959, Quantitative molecular spectroscopy and gas emissivities. Addison-Wesley Co., Reading, Mass
Phillips W.J., 1990, J. Quant. Spec. Rad. Transf. 43, 13
Popova O.P., Nemtchinov I.V., 1996, Meteoritics & Planet. Sci. 31, A110 (Supplement)
Romanov I.S., Stankevich Yu.A., Stanchits L.K., Stepanov K.L., 1993, Thermodynamical Properties, Spectral and Average Absorption Coefficients for Multicomponent Gases in a Wide Range of Parameters. Preprint of Lykov Inst. of Heat and Mass Exchange No. 2, Minsk
Rothman L.S., Gamache R.R., Tipping R.R. et al. 1992, The HITRAN molecular database: editions of 1991 and 1992. J. Quant. Spec. Rad. Transf. 48, 469
Soufiani A., Hartmann J.M., Taine J., 1985, J. Quant. Spec. Rad. Transf. 33, 243
Sulzmann K.G.P., 1973, J. Quant. Spec. Rad. Transf. 13, 931
Svetsov V.V., Nemtchinov I.V., Teterev A.A., 1995, Icarus 116, 131
Tagliaferri E., Spalding R., Jacobs C., Worden S.P., Erlich A., 1994, Detection of meteoroid impacts by optical sensors in Earth orbit. In: Gehrels T. (ed.) Hazards Due to Comets and Asteroids, Univ. Arizona Press, Tucson & London, p. 199
Young S.J., 1977, J. Quant. Spec. Rad. Transf. 18, 29